International Journal of
Recent Innovations in Medicine and Clinical Research
Open Access, Peer Reviewed, Abstracted and Indexed Journal

ISSN: 2582-1075
https://ijrimcr.com/
Volume-4, Issue-3, 2022: 9-26

Research Article

Lipidomic Analysis of the Effects of Melittin on Ovarian Cancer Cells Using Mass Spectrometry

Sanad Alonezi[*1], Valerie A. Ferro[2], David G. Watson[3]

[1]Pharmacy Department, Prince Sultan Military Medical City, Riyadh, Saudi Arabia
[2,3]Strathclyde Institute of Pharmacy and Biomedical Sciences, University of Strathclyde, Glasgow G4 0RE, UK.
[*]Corresponding Author Email: phd-sanad@hotmail.com

Received: May 25, 2022 **Accepted:** June 22, 2022 **Published:** July 6, 2022

Abstract: Lipids help to maintain the integrity of cells, which is the reason for their association with cancer. We hypothesized that the difference in lipid content of ovarian cancer cells sensitive- and resistant to cisplatin might be a useful indirect measure of a variety of functions coupled to ovarian cancer progression. To evaluate the effect of a melittin, a cytotoxic peptide from bee venom with known effects on cell membranes, on the lipid composition of ovarian cancer cell lines A2780 (cisplatin-sensitive) and A2780CR (cisplatin-resistant) a liquid chromatography-mass spectrometry coupled to an Orbitrap Exactive mass spectrometer using an ACE silica gel column was employed. The A2780 and A2780CR cells were treated with 6.8 and 4.5 µg/mL of melittin, respectively. Data extraction with MZmine 2.10 and database searching were applied to provide metabolite lists. PCA and OPLS-DA models were used to assess the different profiles of the lipid composition obtained from the two cell lines. Both models gave clear separation between the treated and untreated samples. In our study, phosphatidylcholine (PC) was the most abundant lipid class in both cell lines, followed by phosphatidylethanolamine (PE), and sphingomyelin. We found a higher level of lipids in ovarian cancer cells sensitive to cisplatin as compared to the resistant cells. Differences in the levels of LysoPC 16:0 and 18:0 were non-significant between cell lines. The changes induced by melittin in both cell lines led mostly to decrease the level of PC and PE lipids. However, the LysoPC level was increased in both cell lines after melittin treatment. The results of the present study show that lipids were significantly altered in both A2780 and A2780CR cells. The observed effect was much more marked in the cisplatin-sensitive cells, suggesting that the sensitive cells undergo much more extensive membrane re-modelling in response to melittin in comparison with the resistant cells.
Keywords: Lipidomic, Melittin, Ovarian cancer, A2780 cells, A2780CR cells, LC-MS.

Introduction

Lipidomics is the science of profiling lipids and forms a subset of metabolomics; it combines technological tools, and especially mass spectrometry, with the principles of analytical chemistry to map on a large scale the lipid composition of a metabolome[1,2]. The contribution made by lipids in cancer pathogenesis is substantial and they have central roles to play in the invasion, migration, and proliferation of cancers[3].

Lipidomics has been studied increasingly in recent years, with particular emphasis on finding lipid indicators of use in diagnosis[4], for targeting drugs[5], and as pharmacological mechanisms[6]. Mass spectrometry has achieved value for assessing changes in lipid metabolism signalling processes mediated by lipids resulting from disease, exposure to toxic substances, gene modification, and drug therapy[7].

A number of mass spectrometry routines are now recognised as a way to elucidate lipid structure[8,9]. In the matter of identifying lipid side chains, the fragmentations providing maximum information come from negative electrospray ionisation (ESI) mode, which generates negative ion fragments thanks to the lipid's fatty acid substituents. In a positive ion mode, phosphocholine (PC) lipid information generated is limited because, due to the phosphatidylcholine head group, the foremost fragmentation mode gives an ion at m/z 184[9].

Lipids have three major roles in cells: they may be structural molecules used to make up membranes, they can provide an important stores of chemical energy, and they play important roles in cell signalling. However, lipids are classified according to the International Lipid Classification and Nomenclature Committee into eight classes, that is, fatty acyls, glycerolipids, glycerophospholipids, sphingolipids, sterol lipids, prenol lipids, saccharolipids, and polyketides[10]. Among the lipids, the phospholipids are possibly one of the most commonly reported in relationship to cancer. During the past few years, elevations in phosphocholine metabolites have been detected in most of the cancers studied[11].

A number of lipid metabolic pathways have been linked to ovarian cancer, particularly those including phospholipids, and fatty acid biosynthesis[11]. One previous study employed mass spectrometry to explore the potential of lysophospholipids, such as lysophosphatidic acid, lysophosphatidylinositol, and lysophosphatidylcholine, as biomarkers for ovarian cancer detection in women with ovarian cancer and healthy controls[12]. Previous studies on ovarian cancer cells have shown that the ovaries are abundant in glycerophospholipids which are a potential signature of ovarian cancer[13-15].

Xu et al. reported that lysophosphatidic acid, which is one of the glycerophospholipids with one fatty acid chain and a phosphate group, as a potential biomarker for ovarian and other gynaecological cancers[16]. A previous study showed that lysophosphatidic acid, lysophosphatidylserine and sphingosylphosphorylcholine all induce transient increases in cytosolic free calcium [Ca^{2+}] in both ovarian and breast cancer cell lines[17]. There is a strong relationship between the calcium and lipid metabolism and cell death. Intracellular calcium homeostasis is extremely important for healthy cells, and the alteration in intracellular calcium homeostasis will lead to cell damage or death[18,19].

Melittin is a major toxin component of honey bee venom that has been reported to exhibit a variety of anticancer applications[20]. The amphipathic property of melittin makes it pass through the phospholipid bilayers of cell membrane and it acts as a surfactant. The interaction between melittin and cell membranes leads to a disruption of the acyl groups of the phospholipids, increased susceptibility to action by phospholipase on the phospholipid, and higher rates of prostaglandin synthesis from arachidonic acid liberated from phospholipid breakdown[21].

Another study showed that FK866 treatment resulted in a significant dose-dependent increase in the glycerophosphocholine levels in A2780 cells[22]. Alteration in glycerophospholipids may be connected with their roles in membrane integrity and mitogenic signal transduction[23]. Moreover, recent studies on metabolic alterations in cancer cells directed into apoptosis reported increased levels of mobile lipids[24,25].

Despite a lipidomic approach having acknowledged value in differentiating between classes and molecular species of phospholipid (PL)[26], most studies focus on only one or a limited number of PL classes and rarely on identifying those lipid molecular species which cancer changes and which could also identify changed metabolic pathways and potential biomarkers. Alonezi et al. reported metabolomic studies based on ovarian cancer cells metabolic profiling related to the effect of melittin on the A2780 and A2780CR[27]. Therefore, the goal of the current study was to extend the metabolomics analysis to lipidomic analysis of ovarian cancer cell lines. With this approach, changes in membrane lipid composition in ovarian cancer cells were identified. The profiling of lipids was

performed by LC-MS using a high performance liquid chromatography (HPLC) system coupled to an Orbitrap Exactive mass spectrometer using an ACE silica gel column.

The selective MS^2 fragmentation of some lipids was carried out by using a HPLC system combined with a LTQ-Orbitrap mass spectrometer. The resulting data were extracted by MZMine and subsequently analysed by univariate and multivariate approaches with SIMCA-P.

Materials and Methods

Cell Lines and Cultures

The cisplatin-sensitive (A2780) and resistant (A2780CR) human ovarian carcinoma cells were obtained from ECACC (Porton Down, Salisbury, UK) and maintained at 75×10^4 cells/mL in RPMI 1640 medium (Lonza, Verviers, Belgium) supplemented with 1% (v/v) L-glutamine (Invitrogen, Paisley, UK), 100 IU/mL/100µg/mL penicillin/streptomycin (Invitrogen, Paisley, UK), and 10% (v/v) foetal bovine serum (FBS) (Life Technologies, Carlsbad, CA).

In addition, the cultures for the A2780CR cells contained 1µm cisplatinum (Tocris Bioscience, Bristol, UK) in the first three passages. Sub-confluent cultures were split by trypsinisation every 4-5 days and maintained at 37^0C in a humidified atmosphere saturated with 5% CO_2.

Cell Viability Assay against Melittin

Melittin was purified from bee venom (supplied by Beesen Co. Ltd, Dae Jeon, Korea) by reversed phase liquid chromatography[28] and reconstituted in sterile water to form a stock solution of 1 mg/mL before storage at -20^0C until required for analysis. Cell viability was assessed by an Alamar Blue (AB) cell viability reagent (Thermo Fisher Scientific, Loughborough, UK) [27]. Both A2780 and A2780CR cells were seeded at 1×10^4 cells/well in 96-well plates (Corning, Sigma-Aldrich) and incubated at 37^0C and 5% CO_2 in a humidified atmosphere for 24 h. After this incubation period, the cells were treated with various concentrations of melittin ranging from 0.5 to 14 µg/mL in 100 µL of medium, and re-incubated at 37^0C and 5% CO_2 for a further 24 h.

Triton X at 1% (v/v) and cell culture media were used as positive and negative controls, respectively. After this, AB was added at a final concentration of 10% (v/v) and the resultant mixture was incubated for a further 4 h at 37^0C and 5% CO_2. Then, the plates were read at an excitation wavelength of 560 nm and the emission at 590 nm was recorded on a SpectraMax M3 microplate reader (Molecular Devices, Sunnyvale, CA). Background-corrected fluorescence readings were converted to cell viability data for each test well by expressing them as percentages relative to the mean negative control value.

Determination of IC_{50}

GraphPad Prism for Windows (version 5.00, GraphPad Software, San Diego, California, USA) was employed to produce dose-response curves by performing nonlinear regression analysis of the cell viability data. The mean inhibitory concentration (IC_{50}) values were calculated from at least three measurements of independent experiments (n=3).

Determination of Effect of Melittin on Cell Lipids Metabolism

The A2780 and A2780CR cell lines were separately treated with melittin at concentrations of 6.8 and 4.5 µg/mL respectively for 24 h (n=4). The cells were seeded at 75×10^4 cells/mL in T-25 cell culture flasks and incubated for 1 doubling time (48 h) before treatment with the melittin and incubation for an additional 24 h. After the treatment, the medium was removed and the cells were washed twice with 3 mL of phosphate-buffered saline (PBS) at 37^0C before lysis.

Lipids were extracted with isopropanol (4^0C) (1 mL per $2x10^6$ cells). The cells were scraped and cell lysates mixed on a Thermo mixer at 1440 rotations per minute (rpm) for 12 min at 4^0C, before being centrifuged at 13500 rpm for 15 min at 0^0C. The supernatants were collected and transferred into

HPLC vials for LC-MS analysis. During the analysis, the temperature of the autosampler was maintained at 4^0C. The pooled quality control (QC) sample were injected in each analysis run in order to facilitate identification and to evaluate the stability and reproducibility of the analytical method, respectively. The pooled QC sample was obtained by taking equal aliquots from all the samples and placing them into the same HPLC vial.

Chromatographic Conditions For Column

An ACE silica gel column (150 x 4.6 mm, 3µm, Hichrom Reading UK) was used to study the effects of melittin on cisplatin resistant and cisplatin sensitive ovarian cancer cell lipids metabolism. The mobile phase for ACE silica gel column consisted of (A) 20% isopropyl alcohol (IPA) in acetonitrile (ACN) (v/v) and (B) 20% IPA in 0.02M ammonium formate (v/v). The flow rate was 0.3 mL/min and gradient was as follows: 0–1 min 8% B, 5 min 9% B, 10 min 20% B, 16 min 25% B, 23 min 35% B, 26–40 min 8% B as described previously[29].

Liquid Chromatography–Mass Spectrometry (LC-MS) Conditions

Liquid chromatographic separation was carried out on an Accela HPLC system interfaced to an Exactive Orbitrap mass spectrometer (Thermo Fisher Scientific, Bremen, Germany). The nitrogen sheath and auxiliary gas flow rates were maintained at 50 and 17 mL/min. The electrospray ionisation (ESI) interface was operated in a positive/negative dual polarity mode. The spray voltage was 4.5 kV for positive mode and 4.0 kV for negative mode, while the ion transfer capillary temperature was 275^0C. Full scan data was obtained in the mass-to-charge ratio (m/z) range of 75 to 1200 for both ionisation modes with settings of AGC target and resolution as Balanced (1E6) and High (50,000) respectively.

Mass calibration was performed for both positive and negative ESI polarities before the analysis using the standard Thermo Calmix solution (Thermo Fisher Scientific, Bremen, Germany) with additional coverage of the lower mass range with signals at m/z 83.0604 (2×ACN+H) for the positive and m/z 91.0037 ($2\times HCOO^-$) for the negative modes respectively. The resulting data were recorded using the XCalibur 2.1.0 software package (Thermo Fisher Scientific, Bremen, Germany).

MS^2 analysis of lipids was carried out on an LTQ Orbitrap using the ACE silica gel column. Instrument settings were as for the Exactive instrument except that the instrument was operated in negative ion mode alone. The PC lipids of interest were analysed in negative ion mode by setting the source collision energy to 35V to remove formic acid and methyl from the formic acid adducts of the molecular ions[29] and then carrying of MS^2 with a collision energy of 35V using the LTQ ion trap as the detector.

Data Extraction and Analysis

Data extraction for each of the samples was carried out by MZmine-2.10 software[30,31]. The extracted ions, with their corresponding m/z values and retention times, were pasted into an Excel macro of the most common metabolites prepared in–house to facilitate identification, and a library search was also carried out against accurate mass data of the metabolites in the Human Metabolome, KEGG, and Metlin databases. The lists of the metabolites obtained from these searches were then carefully evaluated manually by considering the quality of their peaks and their retention time match with to the standard metabolite mixtures run in the same sequence.

Statistical analyses were performed using both univariate and multivariate approaches. The p-values from univariate analysis were adjusted using the Bonferroni correction and differences in the levels (or peak areas) of the metabolites between treated and control cells were considered significant at $p<0.05$. SIMCA-P software version 14.0 (Umetrics, Crewe, UK) was used for unsupervised multivariate analysis of the metabolite data with Pareto scaling prior to principal component (PCA) and hierarchical clustering (HCA) analyses.

Results

The effects of melittin on the lipid composition of ovarian cancer cells (A2780 and A2780CR) were assessed using LCMS and $LCMS^2$ based lipidomics. Differences in the levels of lipids induced by exposure to melittin at concentrations corresponding to IC_{50} with respect to each cell line were assessed.

Multivariate (PCA and OPLS-DA) analyses were used to classify the metabolic phenotypes and identify the differentiating lipids. A clear separation of melittin-treated A2780 and A2780CR cells, and their respective untreated controls, was achieved indicating unique lipid profiles for the treated and control cells with PCA and OPLS-DA models (Figure 1 A and B, respectively).

Pooled quality control (QC) samples were injected in the analysis run in order to quantify the precision of the measurements (Figure 1A). The PCA model parameters were: 4 components, R2X (cum) =0.984; Q2 (cum) = 0.967. The OPLS-DA model parameters and validation of the plot suggested a strong model (R2X (cum) 0.984, R2Y (cum) 0.994, Q2 (cum) 0.984), three components), and the CV-ANOVA for this model was 3.29E-16. Hierarchical clustering analysis of metabolomics data showed distinct separation between the control and treated samples (Figure 2).

There was a very clear separation of the treated versus untreated A2780CR cells obtained by using OPLS-DA model based on the significant metabolites (Figure 3 A). The OPLS-DA model parameters and validation of the plot suggested a strong model (2 components, R2X (cum) = 0.844, R2Y (cum) = 1, Q2 (cum) = 0.988, CV-ANOVA= 1.47E-5). Model validity was verified using permutation tests and receiver operating characteristic (ROC) analysis (Figure S 1, supplementary).

The AUC for a ROC classification is regarded as excellent when AUC > 0.9. The OPLS-DA model classified the treated and untreated A2780 cells into two groups, and the AUC of the ROC for the groups were excellent to perfect classification.

In case of the A2780 cells, OPLS-DA models were also generated by comparing control and treated samples based on the significant metabolites (Figure 3 B). The model parameters and validation of the plot suggested a strong model (R2X (cum) = 0.955, R2Y (cum) = 1, Q2 (cum) = 0.998), two components), and the CV-ANOVA for this model was 4.01E-5. Furthermore, the validity of the ROC and permutation test showed the constructed OPLS-DA model was positive and valid (Figure S 2, supplementary).

For univariate statistical analysis of candidate specific biomarkers in OCC's after exposure to the combinations, the false discovery rate (FDR) was used to reduce the probability of false positive results. There were important differences in lipid composition between the two cell lines before and after treatment with melittin. Changes in various classes of lipids, especially glycerophosphocholines (GPC), glycerophosphoethanolamines (GPE), sphingomyelins, glycerophosphoglycerols (GPG), glycerophosphoinositols (GPI) and glycerophosphoserines (GPS). A list of the putative lipid metabolites is shown in Table 1.

Table 2 and 3 shows a heat map of phosphocholines, phoethanolamines, phosphoinositols, sphingolipid, phosphoglycerols, phosphoserines and diradylglycerols, which are the top 67 lipids by intensity extracted from the A2780 cells in comparison with A2780CR cells. It is clear that the A2780 cell line generally contains more lipids than the A2780CR cell line. The really marked differences between the two cell lines are in several sphingolipids such as dehydrosphinganine and lactosylceramide, and in some ether lipids such as PC36:3, PC36:4, PC38:4 and PC38:6, all of which are lower in the resistant cells.

The level of GPE such as PE38:5 was also found in higher abundance in A2780 cell lines. The differences in lipid composition of the two cell lines suggest that either re-modelling of the cell

membrane might have occurred in order for the A2780CR cells to become resistant, or there is decreased biosynthesis and/or increased utilisation of lipids in cisplatin resistant cells as has been suggested by others[32].

Melittin appears to have some effect on lipid composition in the A2780 cells with the levels of the abundant lipid PC34:1 decreasing, but the effect on this lipid in the A2780CR cells is less marked. Moreover, it was found that treatment of the ovarian cancer cell lines with melittin caused a decrease in PE lipids such as PE34:1 and PE34:2.

Overall there are many changes in lipid abundance in response to melittin but they are generally quite small and restricted to the less abundant lipids. The decrease in the lipids induced by treatment with melittin is less in the case of the A2780CR cells suggesting less membrane damage in the case of these cells.

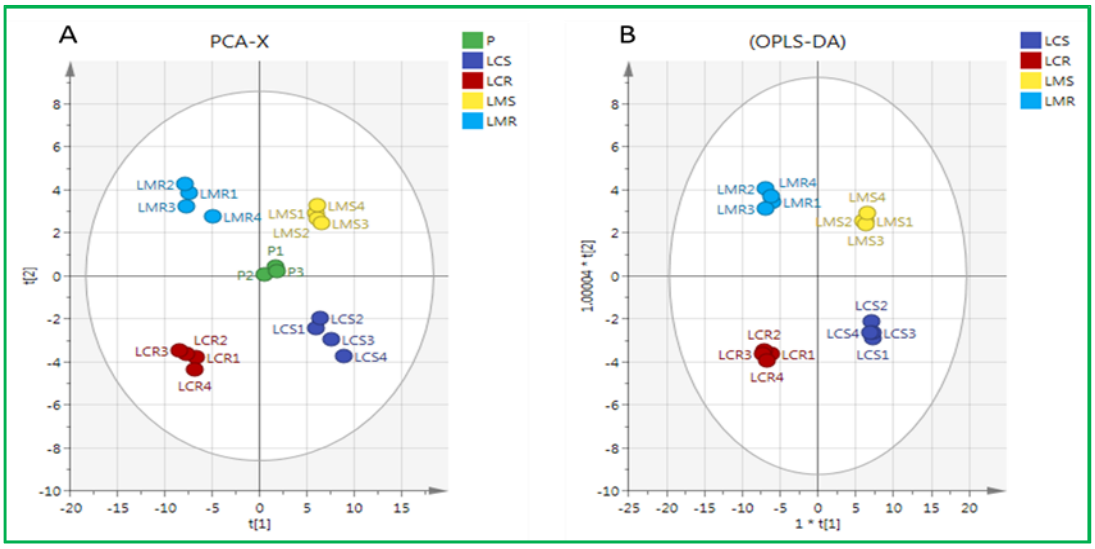

Figure 1. (A) PCA vs (B) OPLS-DA. PCA and OPLS-DA scores plot generated from PCA and OPLS-DA using LC-MS normalized data of cells after exposure to melittin and controls of A2780 and A2780CR cell lines. LMS circles: A2780-treated cells; LCS circles: untreated A2780 cells; LMR circles: A2780CR–treated cells; LCR circles: untreated A2780CR. P circles: Quality control (QC) samples.

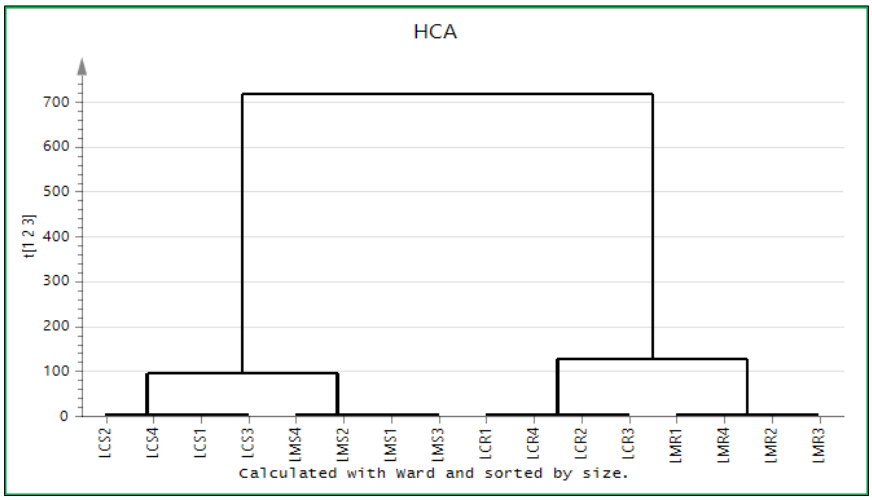

Figure 2. Hierarchical clustering analysis (HCA) of 16 ovarian cancer cell samples. It shows two main groups and four subgroups. The groups: LCR, control of cisplatin resistance cell lines; LMR: A2780CR after treatment with melittin; LCS, control of cisplatin sensitive cell lines; LCS, A2780 after treatment with melittin.

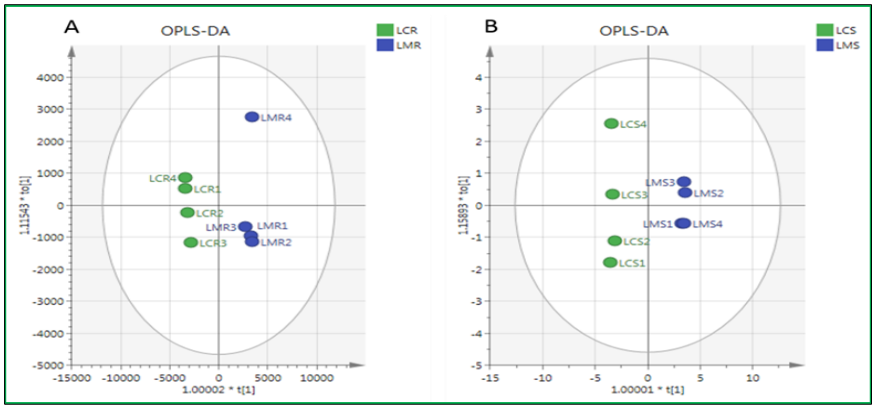

Figure 3. OPLS-DA score plot of (A) A2780CR cell lines before and after treatment with melittin; (B) A2780 cell lines before and after treatment with melittin.

Table 1. Differences in the lipids between A2780 cells and A2780CR cells before and after melittin treatment.

m/z	Rt (min)	Lipid Name	S/R		LMS/LMR		LMR/R		LMS/S	
			P value	Ratio	P value	Ratio	P value	Ratio	P value	Ratio
Sphingolipid (Phosphosphingolipids; Sphingomyelins)										
703.575	14.5	SM (d18:1/16:0)	<0.001	1.875	<0.01	1.723	ns	1.048	ns	0.963
729.590	14.4	SM (d18:1/18:1(9Z))	<0.001	2.756	<0.001	2.587	ns	1.126	ns	1.057
731.606	14.5	SM (d18:0/18:1(9Z))	<0.001	2.969	<0.001	3.069	ns	1.067	ns	1.103
785.652	14.4	SM (d18:1/22:1(13Z))	<0.001	3.042	<0.001	3.099	ns	1.090	ns	1.110
787.668	14.4	SM (d18:1/22:0)	<0.001	3.650	<0.001	3.702	ns	1.049	ns	1.064
813.684	14.4	SM(d18:1/24:1(15Z))	<0.001	1.842	<0.01	1.706	ns	1.068	ns	0.989
Sphingolipid (Sphingoid bases)										
300.289	10.4	3-dehydrosphinganine (3-ketosphinganine)	<0.001	6.209	<0.001	6.634	<0.01	0.616	<0.01	0.659
Sphingolipid (Neutral glycosphingolipids)										
862.624	3.1	LacCer(d18:1/16:0)	<0.001	5.109	<0.001	3.788	ns	1.163	ns	0.862
Sphingolipid (Acidic glycosphingolipids)										
852.587	13.8	(3'-sulfo)Galbeta-Cer(d18:0/20:0(2OH))	<0.001	0.446	<0.01	0.358	ns	0.781	ns	0.626
Glycerophosphoinositols										
887.564	3.6	PI38:3	<0.001	2.321	<0.001	3.662	ns	0.963	<0.01	1.520
883.535	3.5	PI38:5	<0.001	2.469	<0.001	1.603	<0.01	1.727	ns	1.121
835.534	3.8	PI34:1	<0.001	1.751	<0.001	1.449	<0.01	1.977	<0.001	1.635
861.550	3.7	PI36:0	ns	1.026	ns	0.846	<0.01	1.750	<0.01	1.444
887.563	3.5	PI38:4	<0.05	1.169	ns	0.948	<0.01	1.386	<0.05	1.124
Glycerophosphocholines										
706.538	14.1	PC30:0	<0.05	1.307	ns	1.063	<0.01	0.605	<0.01	0.492
704.523	13.9	PC30:1	<0.001	2.664	<0.001	3.037	<0.01	0.472	<0.01	0.538
720.555	14.0	PC31:0	<0.05	1.240	ns	0.805	ns	1.154	<0.05	0.749
732.553	14.0	PC32:1	<0.01	1.874	<0.001	1.756	<0.05	0.594	<0.01	0.557
734.569	14.0	PC32:0	<0.01	1.438	ns	1.100	ns	0.793	<0.01	0.606
730.538	13.9	PC32:2	<0.001	3.790	<0.001	4.606	<0.01	0.578	<0.01	0.703
758.569	13.9	PC34:2	<0.01	1.584	<0.001	1.677	<0.01	0.687	<0.05	0.728
746.605	14.1	PC34:0	<0.001	3.280	<0.001	2.954	ns	0.820	<0.01	0.738
760.584	13.9	PC34:1	<0.05	1.360	ns	1.054	ns	0.824	<0.01	0.639
786.600	13.9	PC36:2	ns	1.097	ns	0.972	ns	0.846	<0.05	0.749
788.615	13.9	PC36:1	ns	0.994	<0.01	0.584	ns	1.111	<0.01	0.653
784.584	13.8	PC36:3	<0.01	1.580	<0.01	1.296	ns	0.930	<0.05	0.763
782.567	13.7	PC36:4	<0.01	1.763	<0.05	1.387	ns	1.204	ns	0.948

808.583	13.7	PC38:5	<0.05	1.636	<0.05	1.411	ns	1.299	ns	1.120
810.599	13.7	PC38:4	<0.01	1.882	ns	0.925	<0.05	1.840	ns	0.905
772.585	13.9	PC35:2	<0.05	1.408	<0.05	1.453	ns	0.902	ns	0.930
814.631	13.9	PC38:2	<0.01	0.666	<0.05	0.493	ns	0.810	<0.01	0.600
774.600	13.9	PC35:1	ns	1.242	ns	0.868	ns	1.205	ns	0.842
838.631	13.7	PC40:4	<0.01	1.783	ns	0.808	ns	1.387	<0.05	0.629
840.647	13.8	PC40:3	ns	1.195	ns	0.862	ns	0.791	<0.01	0.571
842.662	13.8	PC40:2	<0.001	0.573	<0.01	0.430	<0.01	0.661	<0.01	0.496
Glycerophosphocholines										
756.552	13.9	PC34:3	<0.001	2.162	<0.001	2.326	<0.05	0.758	<0.01	0.815
716.559	13.9	PC32:1	<0.001	2.373	<0.01	1.908	ns	1.413	<0.01	1.136
754.537	13.9	PC34:4	<0.001	1.921	<0.001	2.297	<0.01	0.667	<0.01	0.798
496.339	15.0	LysoPC 16:0	ns	1.050	<0.001	0.258	<0.001	5.991	<0.05	1.471
524.371	14.8	LysoPC 18:0	ns	0.847	<0.001	0.173	<0.01	13.157	<0.01	2.695
PC ether lipids										
744.590	13.9	PC34:1 ether lipid	<0.001	1.881	<0.001	1.492	ns	1.188	ns	0.942
794.605	13.8	PC38:5 ether lipid	<0.001	3.578	<0.001	2.011	<0.01	2.115	ns	1.188
796.620	13.8	PC38:4 ether lipid	<0.001	5.719	<0.001	3.027	<0.05	1.730	ns	0.916
770.605	13.9	PC36:2 ether lipid	<0.001	2.704	<0.01	1.585	ns	1.070	<0.01	0.627
692.558	14.2	PC30:2 ether lipid	<0.001	3.447	<0.001	2.796	<0.01	0.767	<0.01	0.622
772.621	14.0	PC36:1 ether lipid	<0.001	2.081	<0.01	1.701	ns	0.975	ns	0.797
774.636	14.1	PC36:0 ether lipid	<0.001	3.398	<0.001	3.110	<0.05	0.758	<0.01	0.694
720.589	14.2	PC32:2 ether lipid	<0.001	4.623	<0.001	5.498	<0.05	0.689	ns	0.820
718.574	14.1	PC32:0 ether lipid	<0.001	3.311	<0.001	2.353	ns	1.167	ns	0.829
768.588	13.8	PC36:3 ether lipid	<0.001	4.563	<0.001	2.746	<0.05	1.621	ns	0.975
766.574	13.7	PC36:4 ether lipid	<0.001	2.545	ns	1.236	<0.01	3.083	<0.01	1.497
792.589	13.7	PC38:6 ether lipid	<0.01	2.357	ns	1.269	<0.05	1.908	ns	1.027
PE ether lipids										
744.553	10.1	PE36:2 ether lipid	ns	0.892	ns	0.824	<0.05	0.746	<0.05	0.689
750.542	9.6	PE38:4 ether lipid	<0.01	1.779	<0.001	1.571	ns	1.044	ns	0.922
724.527	9.7	PE36:5 ether lipid	<0.05	1.510	ns	1.107	<0.05	1.407	ns	1.032
746.569	10.2	PE34:1 ether lipid	<0.01	0.688	<0.01	0.586	ns	0.777	<0.01	0.662
Glycerophosphoethanolamines										
768.552	9.7	PE38:4	<0.001	1.871	<0.001	1.484	<0.01	1.414	ns	1.122
752.558	9.6	PE38:5	<0.001	3.199	<0.001	2.291	<0.05	1.313	ns	0.940
718.538	10.3	PE34:1	ns	1.139	ns	1.077	<0.01	0.610	<0.01	0.577
716.522	10.2	PE 34:2	<0.001	1.652	<0.001	1.861	<0.01	0.543	<0.01	0.612
676.528	10.3	PE 32:0	<0.001	6.850	<0.001	29.351	ns	0.714	<0.001	3.062
704.557	10.3	PE 34:3	<0.001	3.619	<0.001	9.955	ns	0.836	<0.001	2.299
Glycerophosphoglycerols										
721.503	3.7	PG32:0	<0.001	114.589	<0.001	49.988	ns	3.227	<0.05	1.408
775.549	3.7	PG36:1	<0.001	3.688	<0.01	1.573	ns	0.989	<0.01	0.422
773.534	3.5	PG36:2	<0.001	9.482	<0.05	2.057	<0.05	1.782	<0.01	0.387
Glycerophosphoserines										
804.575	14.0	PS37:0	ns	0.965	ns	1.111	ns	1.144	<0.01	1.317
Diacylglycerols										
603.535	3.7	DAG 34:3	<0.001	0.862	<0.01	1.290	<0.001	0.542	<0.01	0.812

PC (Phosphatidylcholine); PE (Phosphatidylethanolamine); PI (Phosphatidylinositol); PG (Phosphatidylglycerol); PS (Phosphatidylserine); DAG (Diacylglycerol); SM (Sphingomyelin); S (A2780 cells); R (A2780CR cells); LMS (melittin treated A2780 cells); LMR (melittin treated A2780CR cells).

Table 2. Heat Map showing the relative abundance of phosphocholine lipids in A2780 (S), A2780CR (R) and melittin treated (LMS and LMR) cells. Red < 2 × 10^5, Yellow > 1× 10^6, Green > 1× 10^7.

m/z	Rt (min)	Lipid Name	Mean S	Mean R	Mean LMS	Mean LMR
706.538	14.1	PC30:0				
704.522	13.9	PC30:1				
720.555	14.0	PC31:0				
732.553	13.9	PC32:1				
734.569	14.0	PC32:0				
730.538	13.9	PC32:2				
758.569	13.8	PC34:2				
746.605	14.1	PC34:0				
760.584	13.9	PC34:1				
786.600	13.9	PC36:2				
788.615	13.9	PC36:1				
784.584	13.8	PC36:3				
782.567	13.7	PC36:4				
808.583	13.7	PC38:5				
810.599	13.7	PC38:4				
772.585	13.8	PC35:2				
814.631	13.8	PC38:2				
774.600	13.9	PC35:1				
838.631	13.7	PC40:4				
840.647	13.8	PC40:3				
842.662	13.8	PC40:2				
756.552	13.8	PC34:3				
716.558	13.9	PC32:1				
754.536	13.9	PC34:4				
496.339	15.0	LysoPC16:0				
524.370	14.9	LysoPC18:0				
766.573	13.7	PC36:4 ether lipid				
744.590	13.9	PC34:1 ether lipid				
794.605	13.8	PC38:5 ether lipid				
796.620	13.8	PC38:4 ether lipid				
770.605	13.9	PC36:2 ether lipid				
692.558	14.2	PC30:2 ether lipid				
772.620	14.0	PC36:1 ether lipid				
774.636	14.1	PC36:0 ether lipid				
720.589	14.2	PC32:2 ether lipid				
718.574	14.1	PC32:0 ether lipid				
768.588	13.8	PC36:3 ether lipid				
792.589	13.7	PC38:6 ether lipid				

Table 3. Heat Map showing the relative abundance of various types of lipid in A2780 (S), A2780CR (R) and melittin treated (LMS and LMR) cells. Red < 2 × 10^5, Yellow > 1× 10^6, Green > 1× 10^7.

m/z	Rt(min)	Lipid Name	Mean S	Mean R	Mean LMS	Mean LMR
703.574	14.5	SM (d18:1/16:0)				
729.590	14.4	SM(d18:1/18:1(9Z))				
731.605	14.5	SM(d18:0/18:1(9Z))				
785.652	14.4	SM(d18:1/22:1(13Z))				
787.668	14.4	SM(d18:1/22:0)				
813.683	14.3	SM(d18:1/24:1(15Z))				
300.289	10.4	3-dehydrosphinganine				
862.624	3.1	LacCer(d18:1/16:0)				
852.587	13.8	(3'-sulfo) Galbeta-Cer (d18:0/20:0(2OH))				
768.552	9.7	PE38:4				
752.558	9.6	PE38:5				
718.538	10.3	PE34:1				
716.522	10.2	PE 34:2				
676.527	10.3	PE 32:0				
704.557	10.3	PE 34:3				
744.553	10.1	PE36:2 ether lipid				
750.542	9.6	PE38:4 ether lipid				
724.527	9.7	PE36:5 ether lipid				
746.569	10.2	PE34:1 ether lipid				
887.564	3.6	PI38:3				
883.534	3.5	PI38:5				
835.534	3.8	PI34:1				
861.550	3.7	PI36:0				
887.563	3.5	PI38:4				
721.503	3.7	PG 32:0				
775.549	3.7	PG 36:1				
773.534	3.5	PG 36:2				
804.575	13.9	PS37:0				
603.534	3.7	DAG 34:3				

MS/MS experiments are used to further identify lipid species or to screen for individual lipid classes. In the case of phosphocholine lipids, in order to avoid the spectrum being dominated by the phosphocholine head group the following method is used. When formate is used in the mobile phase the molecular ions of the negatively charged PC lipids appear as their negatively charged formate adducts. In order to promote the formation of negatively charge ions derived from the acyl chains attached to the glycerol backbone an in source fragmentation energy is applied in negative ion mode. The source fragmentation results in the loss of the formic acid and one of the methyl groups from the choline moiety thus removing the fixed positive charge from the choline head group. The resulting ion is then subjected to further fragmentation by MS/MS or MS^2 in the mass spectrometer. Using this method the fatty acids substituted onto the glycerol backbone are observed as their negatively charged ions. LysoPCs are the phosphocholines that have lost one of the two O-acyl chains, and they

generally have molecular masses in the range of 400–650[33]. Figure 4 shows the MS^2 spectrum of Lysophosphatidylcholines (16:0) and (18:0) in negative ion mode. In this case the MS^2 spectrum is indicative of the palmitic acid and oleic acid within the structure with prominent ions at m/z 255 and 283, respectively. Figure 5 shows the MS^2 spectrum of 18:1/ 18:1 PC in negative ion mode. In this case the MS^2 spectrum is indicative of the acyl groups within the structure with prominent ions at m/z 281 due to the acyl ion $C_{17}H_{33}COO^-$ and at m/z 506 which result from the loss of $C_{18}H_{33}O_2^-$ from the $[M\text{-}CH_3]^-$ ion at m/z 770. In contrast, in positive ion mode the main fragment ion produced is at m/z 184 due to the phosphocholine head group (Figure 6). The PC ether lipids gave diagnostic fragments in MS^2 in negative ion mode. MS^2 in negative ion mode was used to characterise of PC ether lipids 36:4 and 36:3 as shown in Figure 7.

From the information shown in Figure 7 it is apparent that these two lipids both have and an alkyl chain C16:1 and acyl substitutions of C20:4 and C20:5 respectively. The spectra have a common ion at m/z 466 due to neutral loss of the acyl chains from the $[M\text{-}CH_3]^-$ ion. Levels of the 36:4 and 36:3 ether lipids are lower in the resistant cells.

A lactosyl ceramide lipid is lower in the resistant cells. From previous work product ion analysis of the $(M+H)^+$ ions of ceramides reveals cleavage of the amide bond and dehydration of the sphingoid base to form highly abundant, structurally specific O" fragment ions[34]. These product ions yield information regarding the number of carbon atoms in the chain, degree of hydroxylation, unsaturation, or other structural modifications of the long-chain base (e.g., sphingosine, m/z 264; and sphinganine, m/z 266). With this knowledge about the sphingoid base composition and the original precursor m/z, the identity of the fatty acids can be deduced. The lipids were at low levels and the clearest result was obtained by using source induced dissociation (SID). Using ESI-SID in positive mode product ions at m/z 264 and m/z 266 can be used to identify the sphingosine and sphinganine, respectively (Figure 8).

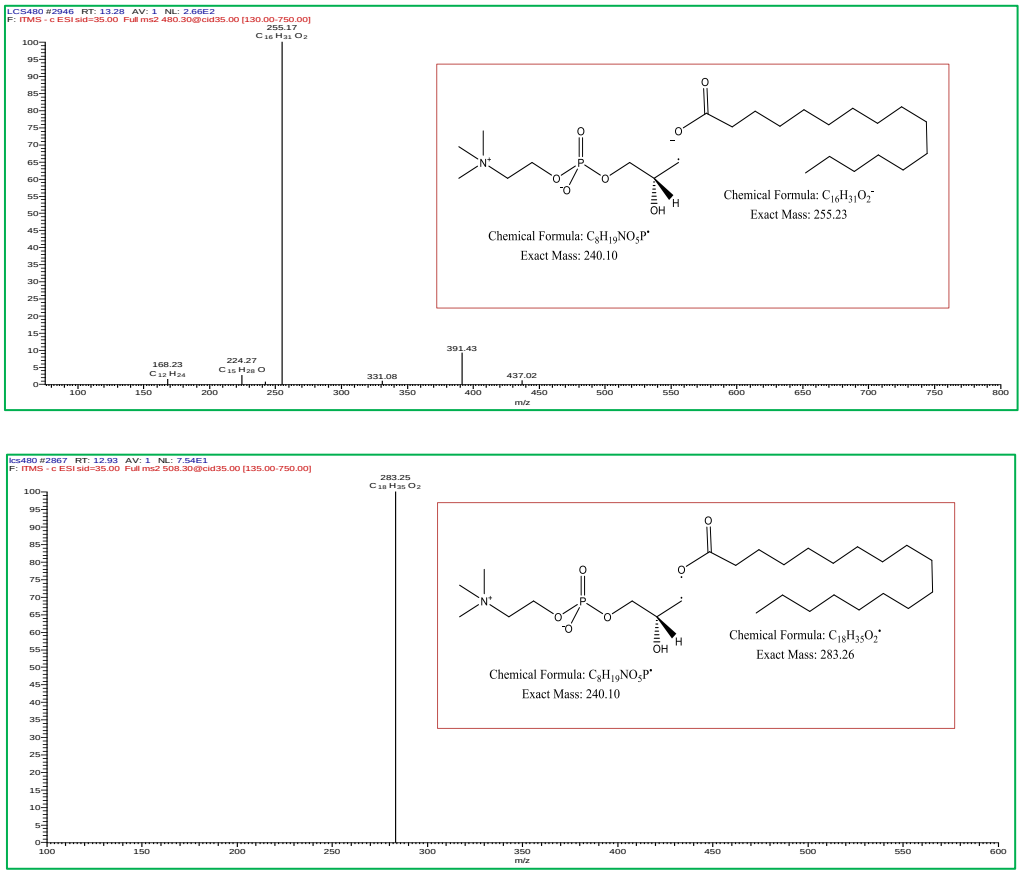

Figure 4. MS^2 spectra of (A) LysoPC 16:0 and (B) LysoPC 18:0 lipid at 35 V following application of a source fragmentation energy of 35 V.

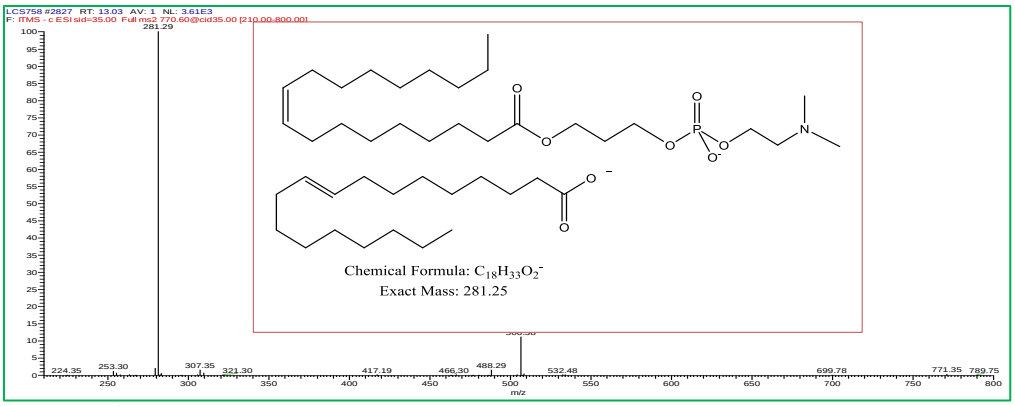

Figure 5. MS^2 spectra of 18:1/18:1 PC lipid at 35 V following application of a source fragmentation energy of 35 V.

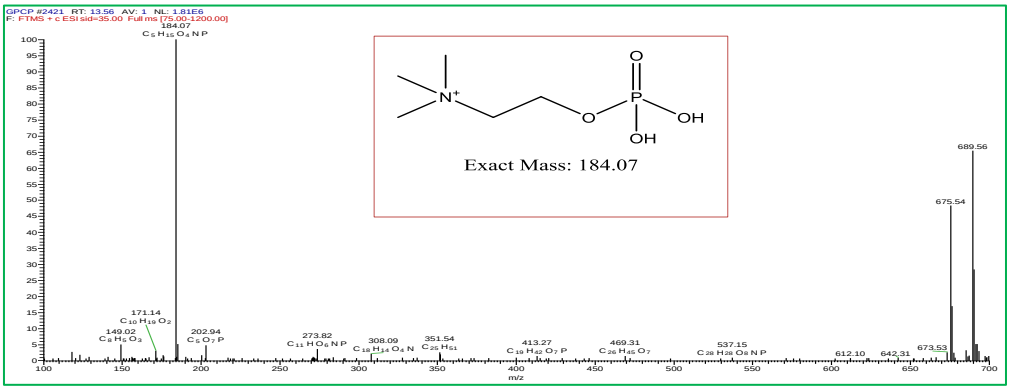

Figure 6. Fragmentation of PC lipids in positive ion mode resulting in m/z 184 due to the phosphocholine head group.

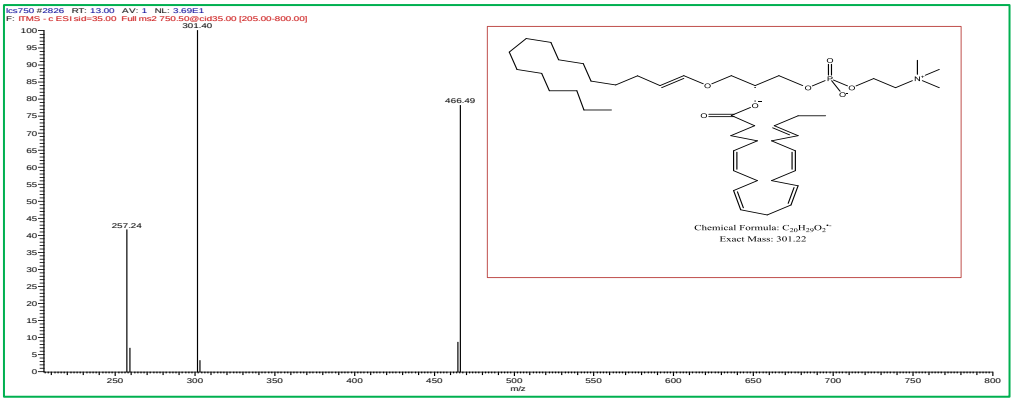

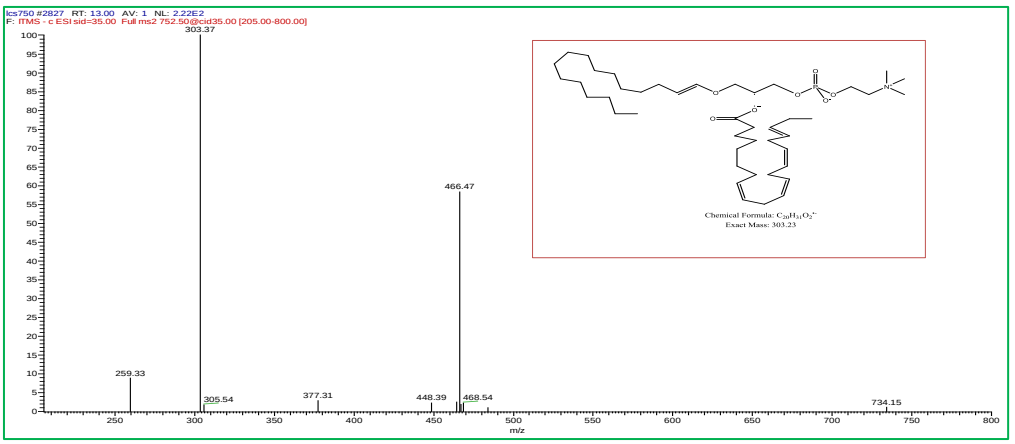

Figure 7. MS^2 spectra of PC ether lipids 36:4 and 36:3 indicate that they are acylated with 20:5 and 20:4 chains respectively.

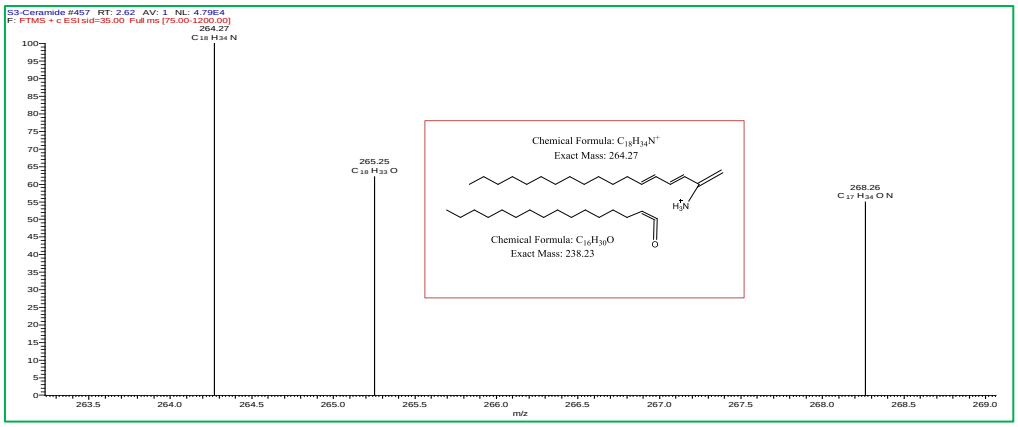

Figure 8. Source induced dissociation spectrum of lactosylceramide (d18:1/16:0) lipid at 35 V.

Figure 9 shows the MS^2 spectrum of 18:0/20:4 PE in negative ion mode. In this case the MS^2 spectrum is indicative of the acyl groups which appear as negatively charged fatty acids at m/z 303 due to $C_{19}H_{31}COO^-$ and at m/z 283 due to $C_{17}H_{35}COO^-$. In the example shown in figure 9 we can also see that there are additional minor fatty acids attached and thus the peak is a mixture of several isomers with different fatty acid chain lengths.

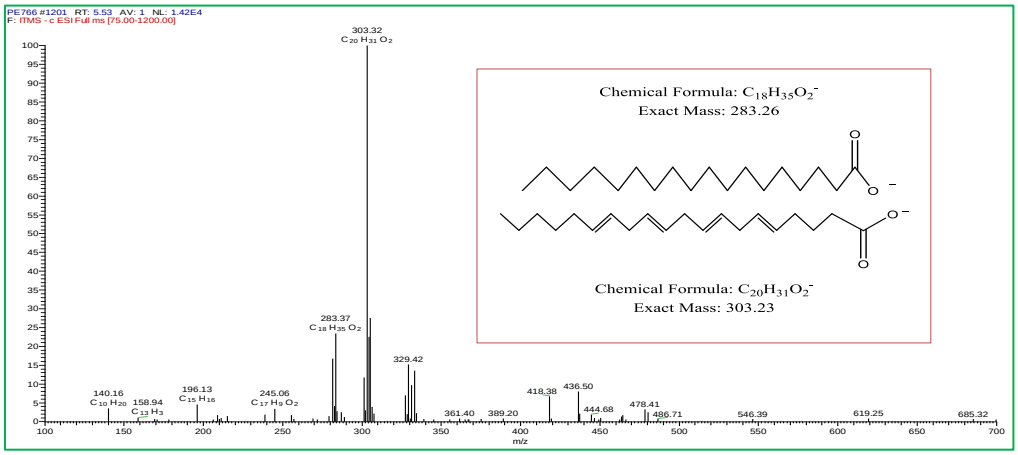

Figure 9. MS^2 spectra of 18:0/20:4 PE lipid.

Discussion

In order to evaluate alterations in the phospholipid profile of human ovarian cancer cells following melittin treatment, mass spectrometry was used to characterise the lipid profiles of A2780 (cisplatin-sensitive) and A2780CR (cisplatin-resistant) cell lines in response to their exposure to melittin. Because of mass spectrometry, we now have much greater access to detailed information concerning cellular lipid composition. ESI-MS has been shown to have an essential role in the characterization, identification, and quantification of lipids[1,35]. Recently, mass spectrometry has been used to determine whether lysophospholipids are useful markers for diagnosis and/or prognosis of ovarian cancer in plasma samples[12]. We have found phosphatidylcholine was the most abundant class lipid class in ovarian cancer cells, followed by phosphatidylethanolamine, phosphatidylinositol, phosphoglycerols, sphingomyelins and phosphoserines. We have also detected a variety of lyso-and ether-linked derivatives of PC and PE.

There are some significant differences in the lipid composition between A2780 and A2780CR cells. The levels of phosphocholine lipids were higher in A2780 cells in comparison to the A2780CR cells. Previous studies also show that an increase in the levels glycerophospholipids could be a signature of ovarian cancer[13-15]. Other studies show that an increase of the level of glycerophosphocholine is the most common feature in a large variety of tumours demonstrating biosynthetic and/or catabolic phosphatidylcholine-cycle pathways of cell membrane turnover[36,37]. Following treatment with

melittin, lipids were significantly altered in both A2780 and A2780CR cells. The effect on lipids is much more marked in that case of the sensitive cells and suggests that the sensitive cells undergo much more extensive membrane re-modelling in response to melittin in comparison with the resistant cells. However, the level of certain species of PC ether lipids were higher in the A2780 cells. For example, PC ether lipids 36:4 and 36:3 were elevated in these cells. The MS^2 spectra of these two lipids (Figure 7) indicate that they are acylated with 20:5 and 20:4 chains respectively. The levels of lyso PCs are also elevated in both cells after exposure to melittin. For example, LPC 16:0 and LPC 18:0 were markedly increased in A2780CR cells following melittin exposure. Fragmentation patterns of these two lipids (Figure 4) indicate of the palmitic acid and oleic acid as the acyl chains. There were no significant differences in those lyso PCs lipid compositions in the untreated A2780 and A2780CR cells. In a previous study it was found that the levels of lysophosphatidic acids were increased in the plasma of ovarian and other gynecologic cancer patients as compared with healthy controls[16].

Moreover, lysophosphatidic acid (LPA) and other lysophospholipids (LPL) such as lysophosphatidylinositol were found useful markers for diagnosis and/or prognosis of ovarian cancer in comparison with healthy control setting[12]. Lyso PC lipids are recycled back into PC lipids via the Land's cycle. The Lands cycle allows remodelling of acyl chains enabling modification of the fatty acid composition of phospholipids that derive from the Kennedy pathway[38]. The process involves alteration of the fatty acyl composition at the sn-2-position of PC resulting in generation of varied PC species with unique fatty acids, each with a different carbon chain length and degree of saturation[39,40,41]. Thus our observations suggest that sensitive cells incorporate LPCs into their membranes faster than the resistant cells and thus remodel their membrane more quickly.

Phosphatidylethanolamine (PE) is a phospholipid found in all living organisms. Most biological membranes are made up of PE together with phosphatidylcholine (PC), phosphatidylserine (PS) and phosphatidylinositol (PI). The levels of several phosphatidylethanolamines such as PE 38:4, PE 38:5, PE 32:0 and PE 34:3 were higher in sensitive cells in comparison to the resistant cells. Furthermore, higher phosphatidylethanolamine and phosphatidylcholine levels in A2780 cells suggest increases in the *de novo* synthesis of these GPLs[42]. Our findings are resemble those from a previous study in which the level of glycerophospholipids were increased as a signature of ovarian cancer[13,14]. Phosphatidylethanolamine can provide a substrate for phosphatidylcholines, whose extreme elevation has previously been observed in ovarian carcinomas[13,15]. There may be a connection between alteration in GPLs and the part they play in membrane integrity and transduction of mitogenic signals[23].

Furthermore, an association has been seen between an increase in phosphatidylinositol and deregulation of the phosphoinositide-3 kinase (PI3K) pathway, which leads in its turn to carcinogenesis and angiogenesis[15]. Phosphoethanolamine, is a substrate for many cell membrane phospholipids that has recently been shown to induce both cell cycle arrest and apoptosis in cancer cells[43,44]. Here, intracellular phosphoethanolamine levels for PE 34:1 and PE 34:2 were decreased in both cell lines after exposure to melittin. In contrast, the level of some PE lipids such as PE 32:0 and PE 34:3 were found increased in A2780 following melittin treatment. Moreover, the levels of PE 38:4 and PE 38:5 were increased in A2780CR cells. This effect could be indicative of increased phospholipid membrane turnover or an apoptotic response to the increasing stress levels.

Several sphingomyelin (SM) lipids are higher in the A2780 cells in comparison to the A2780CR cells. This differs from previous reports of increased ceramide lipids, particularly glucosylceramides and galactosylceramides, in multidrug resistant ovarian cancer cells[45] and breast cancer cells[46]. However, in these previous studies ceramides or glycosylceramides were measured rather than sphingomyelin lipids. Another study showed increases of dihydroceramide, ceramide, sphingomyelin, lactosylceramide, and ganglioside species in ovarian cancer (A2780) cells that had been exposed to synthetic retinoids[47]. In common with Veldman et al.[45], we have seen that resistant

cells contained lower levels of lactosylceramide. Lactosylceramide was characterized by identification of the ions obtained by MS^2 (Figure 8).

That many lipids are present in lower levels in resistant cells, and especially lipids whose function includes promotion of membrane stability, indicates the possibility that resistance to cisplatin is unconventional in this cell line. Cisplatin is a polar drug which crosses cell membranes through the action of organic cation transporters (several of which have been identified) and not by passive diffusion[48]. Thus it is possible that cisplatin resistance could be mediated through mechanisms other than augmentation of membrane lipids. This possibility is supported by two of our findings which suggest that melittin, an agent known to destabilise cell membranes, was more active on the cisplatin resistant compared to cisplatin sensitive cells, and that polyamines were higher in the sensitive cells as described previously[27,49]. Both observations further illustrate the fact that the A2780 cell line may have a more stable cell membrane. Following treatment with melittin, lipids were significantly altered in both A2780 and A2780CR cells. The observed effect was much more marked in the cisplatin-sensitive cells, suggesting that the latter undergo much more extensive membrane re-modelling in response to melittin in comparison with the resistant cells.

Conclusions

Lastly, it will be important to investigate the lipid metabolism as modulators of cell membrane integrity. This study shows that the cisplatin sensitive A2780 cells contain relatively higher levels of sphingolipid and phosphocholine ether lipids which might result in increased membrane stability and repair and thus resistance to the lytic action of melittin in comparison with the cisplatin resistant A2780CR cells. After exposure to melittin, the levels of most of the significantly affected lipid metabolites, particularly phosphocholines (e.g. PC34:0, PC34:1, PC36:1, PC36:2, PC36:3, PC40:3, PC40:4), were lower in A2780 compared to A2780CR cells, suggesting different metabolic responses in the two cell lines.

The higher levels of glycerophosphocholine in A2780 cells may be related to higher *de novo* lipid synthesis and re-direction of cellular metabolism. Given that melittin interacts with cell membranes, the observed effect of greater toxicity of melittin to the resistant cells might suggest that the membranes are less adaptable in the cisplatin resistant cells compared to the sensitive ones. Over all, this study shows that a LC-MS based metabolomics approach for the assessment of drug effects *in vitro* provides a powerful tool for obtaining insights into the mechanism of action of potential therapeutic agents, while offering the possibility to identify key metabolite markers for *in vivo* monitoring of tumour responsiveness to standard chemotherapy. Melittin might serve as a valuable adjuvant in cancer chemotherapy for overcoming chemoresistance.

Supplementary Materials: Figure S 1, Model validity was verified using permutation tests and receiver operating characteristic (ROC) analysis. Figure S 2 showed the validity of the ROC and permutation test.

Acknowledgments: S.A. is funded by the government of Saudi Arabia (Medical Services Ministry of Defence). We thank Beesen Co. Ltd. through a partnership between Strathclyde University and Korea Institute for Advancement of Technology (KIAT).

Conflicts of Interest: The authors declare no conflict of interest.

References

1. Han X, Gross RW. Global analyses of cellular lipidomes directly from crude extracts of biological samples by ESI mass spectrometry: a bridge to lipidomics. J Lipid Res. 2003;44(6):1071-9.
2. Wenk MR. Lipidomics: new tools and applications. Cell. 2010;143(6):888-95.

3. Fernandis AZ, Wenk MR. Lipid-based biomarkers for cancer. J Chromat B. 2009;877(26):2830-5.
4. Wenk MR. Lipidomics in drug and biomarker development. Exp Opin Drug Dis. 2006;1(7):723-36.
5. Maréchal E, Riou M, Kerboeuf D, Beugnet F, Chaminade P, Loiseau PM. Membrane lipidomics for the discovery of new antiparasitic drug targets. Trend Parasitol. 2011;27(11):496-504.
6. Adibhatla RM, Hatcher JF, Dempsey RJ. Lipids and lipidomics in brain injury and diseases. AAPS J. 2006;8(2):E314-21.
7. Watkins SM, Reifsnyder PR, Pan HJ, German JB, Leiter EH. Lipid metabolome-wide effects of the PPARγ agonist rosiglitazone. J Lipid Res. 2002;43(11):1809-17.
8. Li L, Han J, Wang Z, Liu JA, Wei J, Xiong S, Zhao Z. Mass spectrometry methodology in lipid analysis. Int J Molec Sci. 2014;15(6):10492-507.
9. Pulfer M, Murphy RC. Electrospray mass spectrometry of phospholipids. Mass Spectrom Rev. 2003;22(5):332-64.
10. Fahy E, Subramaniam S, Murphy RC, Nishijima M, Raetz CR, Shimizu T, Spener F, van Meer G, Wakelam MJ, Dennis EA. Update of the LIPID MAPS comprehensive classification system for lipids. J Lipid Res. 2009;50:S9-14.
11. Tania M, Khan MA, Song Y. Association of lipid metabolism with ovarian cancer. Curr Oncol. 2010;17(5):6-11.
12. Sutphen R, Xu Y, Wilbanks GD, Fiorica J, Grendys Jr EC, LaPolla JP, Arango H, Hoffman MS, Martino M, Wakeley K, Griffin D. Lysophospholipids are potential biomarkers of ovarian cancer. Can Epidem Biomar Prev. 2004;13(7):1185-91.
13. Iorio E, Mezzanzanica D, Alberti P, Spadaro F, Ramoni C, D'Ascenzo S, Millimaggi D, Pavan A, Dolo V, Canevari S, Podo F. Alterations of choline phospholipid metabolism in ovarian tumor progression. Can Res. 2005;65(20):9369-76.
14. Ben Sellem D, Elbayed K, Neuville A, Moussallieh FM, Lang-Averous G, Piotto M, Bellocq JP, Namer IJ. Metabolomic characterization of ovarian epithelial carcinomas by HRMAS-NMR spectroscopy. J Oncol. 2011;174019.
15. Halama A, Guerrouahen BS, Pasquier J, Diboun I, Karoly ED, Suhre K, Rafii A. Metabolic signatures differentiate ovarian from colon cancer cell lines. J Translat Med. 2015;13(1):223.
16. Xu Y, Shen Z, Wiper DW, Wu M, Morton RE, Elson P, Kennedy AW, Belinson J, Markman M, Casey G. Lysophosphatidic acid as a potential biomarker for ovarian and other gynecologic cancers. Jama. 1998;280(8):719-23.
17. Oliver SG, Winson MK, Kell DB, Baganz F. Systematic functional analysis of the yeast genome. Trends Biotechnol. 1998;16(9):373-8.
18. Mattson MP, Chan SL. Calcium orchestrates apoptosis. Nat Cell Biol. 2003;5(12):1041-3.
19. Garcia-Prieto C, Ahmed KB, Chen Z, Zhou Y, Hammoudi N, Kang Y, Lou C, Mei Y, Jin Z, Huang P. Effective killing of leukemia cells by the natural product OSW-1 through disruption of cellular calcium homeostasis. J Biolog Chem. 2013;288(5):3240-50.
20. Gajski G, Garaj-Vrhovac V. Melittin: a lytic peptide with anticancer properties. Environ Toxicol Pharmacol. 2013;36(2):697-705.
21. Mufson RA, Laskin JD, Fisher PB, Weinstein IB. Melittin shares certain cellular effects with phorbol ester tumour promoters. Nature. 1979;280(5717):72-4.

22. Tolstikov V, Nikolayev A, Dong S, Zhao G, Kuo MS. Metabolomics analysis of metabolic effects of nicotinamide phosphoribosyltransferase (NAMPT) inhibition on human cancer cells. PloS One. 2014;9(12):e114019.

23. Ackerstaff E, Glunde K, Bhujwalla ZM. Choline phospholipid metabolism: a target in cancer cells?. J Cell Biochem. 2003;90(3):525-33.

24. Milkevitch M, Shim H, Pilatus U, Pickup S, Wehrle JP, Samid D, Poptani H, Glickson JD, Delikatny EJ. Increases in NMR-visible lipid and glycerophosphocholine during phenylbutyrate-induced apoptosis in human prostate cancer cells. Biochimica et Biophysica Acta (BBA)-Mol Cell Biol Lip. 2005;1734(1):1-12.

25. Rainaldi G, Romano R, Indovina P, Ferrante A, Motta A, Indovina PL, Santini MT. Metabolomics using 1H-NMR of apoptosis and Necrosis in HL60 leukemia cells: differences between the two types of cell death and independence from the stimulus of apoptosis used. Radiat Res. 2008;169(2):170-80.

26. Milne S, Ivanova P, Forrester J, Brown HA. Lipidomics: an analysis of cellular lipids by ESI-MS. Meth. 2006;39(2):92-103.

27. Alonezi S, Tusiimire J, Wallace J, Dufton MJ, Parkinson JA, Young LC, Clements CJ, Park JK, Jeon JW, Ferro VA, Watson DG. Metabolomic profiling of the effects of melittin on cisplatin resistant and cisplatin sensitive ovarian cancer cells using mass spectrometry and biolog microarray technology. Metabol. 2016;6(4):35.

28. Tusiimire J, Wallace J, Dufton M, Parkinson J, Clements CJ, Young L, Park JK, Jeon JW, Watson DG. An LCMS method for the assay of melittin in cosmetic formulations containing bee venom. Analyt Bioanal Chem. 2015;407(13):3627-35.

29. Zheng L, T'Kind R, Decuypere S, von Freyend SJ, Coombs GH, Watson DG. Profiling of lipids in Leishmania donovani using hydrophilic interaction chromatography in combination with Fourier transform mass spectrometry. Rapid Commun Mass Spectro. 2010;24(14):2074-82.

30. Pluskal T, Castillo S, Villar-Briones A, Orešič M. MZmine 2: modular framework for processing, visualizing, and analyzing mass spectrometry-based molecular profile data. BMC Bioinfor. 2010;11:395.

31. Katajamaa M, Orešič M. Processing methods for differential analysis of LC/MS profile data. BMC Bioinfor. 2005;6:179.

32. Poisson LM, Munkarah A, Madi H, Datta I, Hensley-Alford S, Tebbe C, Buekers T, Giri S, Rattan R. A metabolomic approach to identifying platinum resistance in ovarian cancer. J Ovar Res. 2015;8:13.

33. Dutta A, Shetty P, Bhat S, Ramachandra Y, Hegde S. A mass spectrometric study for comparative analysis and evaluation of metabolite recovery from plasma by various solvent systems. J Biomol Tech. 2012;23:128.

34. Merrill Jr AH, Sullards MC, Allegood JC, Kelly S, Wang E. Sphingolipidomics: high-throughput, structure-specific, and quantitative analysis of sphingolipids by liquid chromatography tandem mass spectrometry. Meth. 2005;36(2):207-24.

35. Welti R, Wang X. Lipid species profiling: a high-throughput approach to identify lipid compositional changes and determine the function of genes involved in lipid metabolism and signaling. Curr Opin Plant Biol. 2004;7(3):337-44.

36. Hishikawa D, Hashidate T, Shimizu T, Shindou H. Diversity and function of membrane glycerophospholipids generated by the remodeling pathway in mammalian cells. J Lipid Res. 2014;55(5):799-807.

37. McLean MA, Priest AN, Joubert I, Lomas DJ, Kataoka MY, Earl H, Crawford R, Brenton JD, Griffiths JR, Sala E. Metabolic characterization of primary and metastatic ovarian cancer by 1H- MRS in vivo at 3T. Mag Reson Med. 2009;62:855-61.

38. Wang L, Shen W, Kazachkov M, Chen G, Chen Q, Carlsson AS, Stymne S, Weselake RJ, Zou J. Metabolic interactions between the Lands cycle and the Kennedy pathway of glycerolipid synthesis in Arabidopsis developing seeds. Plant Cell. 2012;24(11):4652-69.

39. Shimizu T, Ohto T, Kita Y. Cytosolic phospholipase A2: biochemical properties and physiological roles. IUBMB Life. 2006;58(5- 6):328-33.

40. Schlame M, Rua D, Greenberg ML. The biosynthesis and functional role of cardiolipin. Prog Lipid Res. 2000;39(3):257-88.

41. Lands WE. Stories about acyl chains. Biochimica et biophysica Acta- Molec Cell Biol Lip 2000;1483(1):1-4.

42. Budczies J, Denkert C, Müller BM, Brockmöller SF, Klauschen F, Györffy B, Dietel M, Richter-Ehrenstein C, Marten U, Salek RM, Griffin JL. Remodeling of central metabolism in invasive breast cancer compared to normal breast tissue–a GC-TOFMS based metabolomics study. BMC Genom. 2012;13:334.

43. Ferreira AK, Freitas VM, Levy D, Ruiz JL, Bydlowski SP, Rici RE, Filho OM, Chierice GO, Maria DA. Anti-angiogenic and anti-metastatic activity of synthetic phosphoethanolamine. PLoS One. 2013;8(3):e57937.

44. Ferreira AK, Meneguelo R, Pereira A, R Filho OM, Chierice GO, Maria DA. Synthetic phosphoethanolamine induces cell cycle arrest and apoptosis in human breast cancer MCF-7 cells through the mitochondrial pathway. Biomed Pharmacother. 2013;67(6):481-7.

45. Veldman RJ, Klappe K, Hinrichs J, Hummel IN, Van Der Schaaf G, Sietsma H, Kok JW. Altered sphingolipid metabolism in multidrug- resistant ovarian cancer cells is due to uncoupling of glycolipid biosynthesis in the Golgi apparatus. FASEB J. 2002;16(9):1111-3.

46. Lavie Y, Cao HT, Bursten SL, Giuliano AE, Cabot MC. Accumulation of glucosylceramides in multidrug-resistant cancer cells. J Biolog Chem. 1996;271(32):19530-6.

47. Valsecchi M, Aureli M, Mauri L, Illuzzi G, Chigorno V, Prinetti A, Sonnino S. Sphingolipidomics of A2780 human ovarian carcinoma cells treated with synthetic retinoids. J Lipid Res. 2010;51(7):1832-40.

48. Yonezawa A, Inui KI. Organic cation transporter OCT/SLC22A and H+/organic cation antiporter MATE/SLC47A are key molecules for nephrotoxicity of platinum agents. Biochem Pharmacol. 2011;81(5):563-8.

49. Al Shehri A, Khan S, Shamsi S, Almureef SS. Comparative study of mulligan (SNAGS) and Maitland mobilization in neck pain. Europ J Phys Edu Sport Sci. 2018;5(1):19-29.

Citation: Alonezi S, Ferro VA, Watson DG. Lipidomic Analysis of the Effects of Melittin on Ovarian Cancer Cells Using Mass Spectrometry. Int J Rec Innov Med Clin Res. 2022;4(3):9-26.